

Article

Past and Present Drivers of Karst Formation of Ciénega de El Mangle, Panama

Jaime Rivera-Solís ^{1,2}, Adolfo Quesada-Román ^{3,*} and Fran Domazetović ⁴

¹ Centro de Capacitación, Investigación y Monitoreo de la Biodiversidad (CCIMBIO-CRUV-UP), Centro Regional Universitario de Veraguas (CRUV), Universidad de Panamá, Transistmica 0923, Panamá; jaime.rivera@up.ac.pa

² Departamento de Geografía Física, Universidad de Panamá, Transistmica 0923, Panamá

³ Laboratorio de Geografía Física, Escuela de Geografía, Universidad de Costa Rica, San José 2060, Costa Rica

⁴ Center for Geospatial Technologies, Department of Geography, University of Zadar, 23000 Zadar, Croatia; fdomazeto@unizd.hr

* Correspondence: adolfo.quesadaroman@ucr.ac.cr

Abstract: Tropical coastal karst areas represent dynamic, fragile, and biodiverse environments. Central America's karst regions have been scarcely studied, with most of the research focused on the northern part of the region and on several larger cave systems. The coastal carbonate zones of the Central American region represent a unique karstic landscape, which, so far, has been insufficiently studied. Therefore, in this paper, we aim to describe the (i) landscape geomorphology and (ii) chemical conditions that define Ciénega de El Mangle in Panama as a distinctive karstic site. Carried geomorphological mapping and the characterization of karstic features have resulted in the identification of the different karstic forms and processes that are present within this unique karstic area. Considering that the chosen karstic study area is located in a marine-coastal fringe on the periphery of a lagoon, it is affected by a combination of several factors and processes, including seawater intrusion (through sinkholes), the formation of conchiferous limestone (CaCO₃), and NaCl precipitation related to efflorescence. Due to the seasonally humid tropical climate, the chemical weathering processes are intense, thus forming alkaline soils that are hindering the development of mangrove vegetation. The geomorphology of the area results from intense evaporation combined with an influx of brackish groundwater, due to which a landscape has evolved in the marine-coastal strips, of seasonal tropical climates, that exhibit saline beaches, known as a littoral shott. In total, 24 karstic microdolines have evolved within the shott, of which six represent domical geoforms formed by gradual evaporitic precipitation, while seven other geoforms represent active karstic sinkholes filled with brackish water. These results are key for understanding the past and present climate interactions and conditions that have led to the formation of tropical karst environments.

Keywords: tropical coastal karst; Central America; karstic landscape; fossiliferous limestone; evaporites; sinkholes; microdolines



Citation: Rivera-Solís, J.; Quesada-Román, A.; Domazetović, F. Past and Present Drivers of Karst Formation of Ciénega de El Mangle, Panama. *Quaternary* **2023**, *6*, 58. <https://doi.org/10.3390/quat6040058>

Academic Editor: Gemma Aiello

Received: 17 August 2023

Revised: 25 October 2023

Accepted: 23 November 2023

Published: 29 November 2023



Copyright: © 2023 by the authors. Licensee MDPI, Basel, Switzerland. This article is an open access article distributed under the terms and conditions of the Creative Commons Attribution (CC BY) license (<https://creativecommons.org/licenses/by/4.0/>).

1. Introduction

Sediments deposited in marginal marine environments present distinct geochemical, mineralogical, and micropalaeontological components due to the variability of physical and chemical conditions [1]. Most karstic forms depend directly or indirectly on the chemical weathering—karstification—of soluble rocks marked by a high degree of permeability due to secondary porosity [2]. Studies of marginal marine environments are necessary in palaeoenvironmental research, especially related to sea level changes [3]. The karstic geomorphologic system differs from others due to the dominant role of dissolution, which results in subsurface rather than surface water flow [4].

Globally, carbonate rocks suitable for karstification form 15.2% of all ice-free land surfaces, as well as 15.7% of global coastlines [4,5]. While karst is present in all climatic

zones, about 8.8% of all karstifiable land surfaces are located within tropical climates [5]. In Central America, karst environments are located mostly in the northern part of the region but are present throughout the study area [6]. The largest karst area in Central America covers the Yucatán Peninsula in Mexico and parts of Guatemala and Belize; here, a large karst aquifer system is characterized by many collapsed dolines, locally called cenotes [7,8]. Furthermore, cone and tower karst are also common in northern Central America, especially in Guatemala and Honduras, while doline karst is typical of the limited zones of Nicaragua, Costa Rica, and Panama [9]. Among the common landforms in the region are karstic hills (cones, cockpit, and tower types), sinkholes, caves, and other subsidence or collapse structures, such as underground rivers [10]. Panama and the Azuero peninsula present doline and fluviokarst [6].

Karst areas represent a fragile environment that is susceptible to various anthropogenic and natural pressures [11,12]. Karst landscapes face natural pressures like rock dissolution and sinkhole formation alongside anthropogenic hazards including urbanization, mining, agriculture, tourism, pollution, deforestation, and invasive species [13,14]. The lack of proper management in karst areas can lead to several issues, such as soil erosion [15,16], aquifer pollution, subsidence [17–19], and collapse [12]. Studying karstic depressions is vital for understanding groundwater dynamics and land stability, offering valuable insights into water resource management and geohazard mitigation [20–22]. Therefore, detailed knowledge of karstic areas is crucial for the sustainable management and evasion of environmental problems in the future, as well as for the improvement of landscape and land use planning [23–26].

In this paper, we hypothesize that Ciénega de El Mangle in Panama has unique karstic characteristics that must be recognized through fieldwork and landscape geomorphological mapping, as well as through climatic and chemical assessment. Hence, we aim to characterize (i) the landscape geomorphology and (ii) the chemical conditions that define Ciénega de El Mangle in Panama as an exceptional karstic depression site. This study will improve the overall knowledge about karst environments in Central America, a region that lacks geomorphological data, especially in regard to the coastal carbonate zones.

2. Materials and Methods

2.1. Geographical Context of Study Area

The study site is located at the geographical coordinates 8.1202955 N and –80.55578616 West (Figure 1), on the Azuero Peninsula, at the southern part of the Isthmus of Panama. Geographical context is very important for distinguishing the impacts of morphogenetic processes on the formation of current natural conditions within the chosen study site. Therefore, the following part of this manuscript is aimed at the explanation of different physical–geographical variables at the regional and local scales, including the tectonic, geological, climatic, geomorphological, edaphic, and phytogeographical characteristics.

In a general context, Panama lies on a tectonic block (microplate), bordered to the north by the Caribbean plate, to the east by the South American plate, to the west by the Cocos plate, and to the south by the Nazca plate; the last is bordered by the Mesoamerican Trench to the southwest and the Panama Trench to the south–southeast [27]. Consequently, the area of the Azuero Peninsula is characterized by seismic events associated with a set of parallel faults (Tonosí and Azuero-Soná) with left-lateral displacement [28]. Thus, the tectonic microplate is made up of the Chorotega block (the western region of the country) and the Chocó block (eastern region), which are composed predominantly of mafic igneous rocks—oceanic ophiolites and flints associated with siliceous limestones. These igneous blocks contrast the large sedimentary basins that extend peripherally throughout the Gulf of Panama, including the Parita Bay [29] and especially the area of the lower basin of the Santa María River, which is geologically constituted by Quaternary sediments and reefs [30].

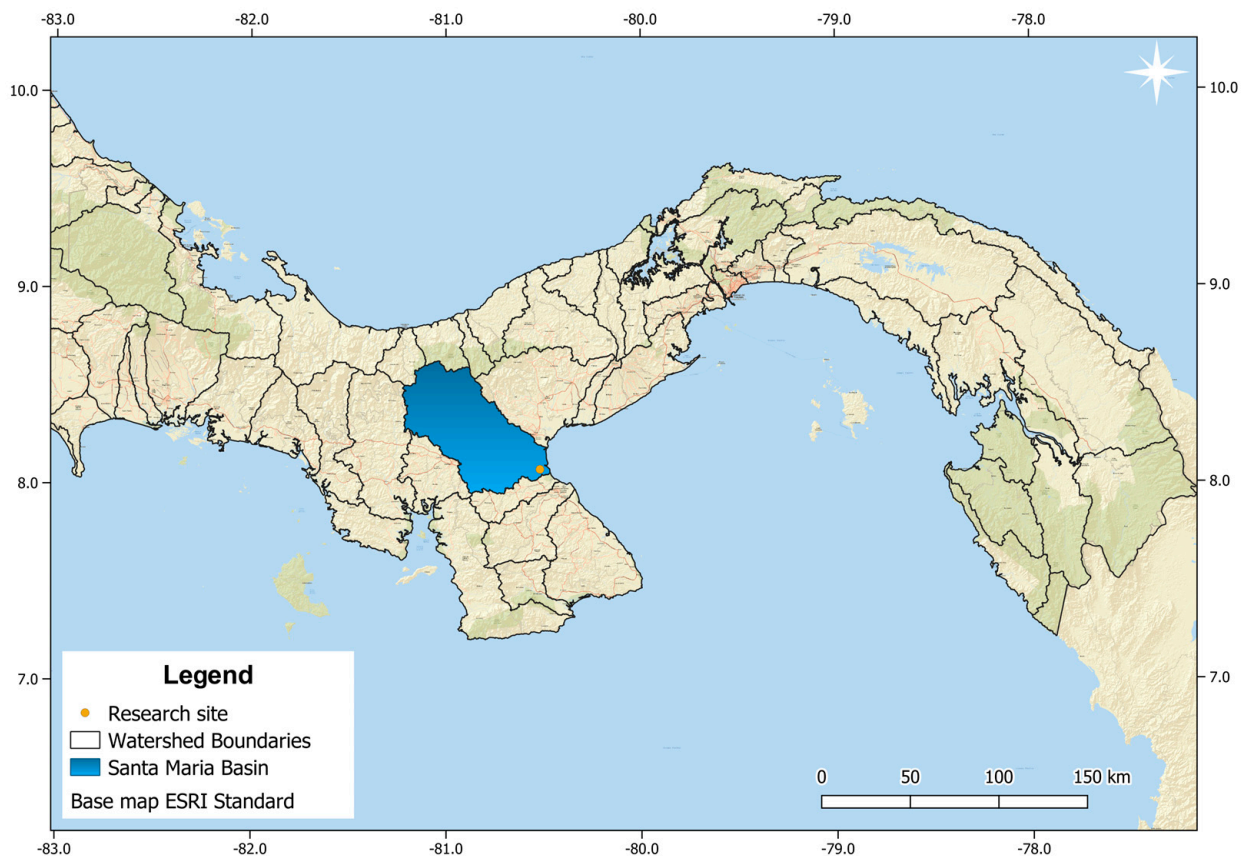


Figure 1. Location of the study site in the Panamanian context.

The geotectonic processes that created the isthmus began in the late Cretaceous (63 Ma) and were completed in the late Pliocene and early Pleistocene [29]. However, recently collected fossil evidence from the canal area suggests that North America was connected to central Panama in the early to mid-Miocene [31]. Consequently, diverse geomorphic processes propitiate the evolution of the isthmus. Continuous episodes of magmatic flow and tectonic uplift gave rise to the Central Cordillera that reaches 3475 m asl (Tabasará and Veraguas mountain ranges) towards the central-western sector, while other subvolcanic intrusions led to the development of mountains and mountain ranges towards the east and south of the isthmus. Then, the weathering of these surfaces by both physicochemical weathering and erosion (according to the morphogenetic environment) leads to the formation of hills that appear in wide coastal plains towards the Pacific sector [32]. The colder climate during the ice age turned the tropical forests of the isthmus into drier environments, favoring the development of wide savannas after the regression of the sea level for approximately 100 m [31].

Tropical climate conditions in this region are modulated by the influence of the Intertropical Convergence Zone, trade winds, tropical cyclones, cold fronts, and El Niño—Southern Oscillation [32,33]. Regarding its climatic characteristics, which definitely determine the celerity of morphogenetic processes and influence the conformation of the soil and vegetation cover, the Last Glacial period of the northern hemisphere induced the absence of summer rains in the tropics; for such a reason, the climate of Panama was colder and more arid than the current one, causing the reduction in tropical forests and biotic renewal [31,33]. However, today, attending the quantitative limits of Köppen–Geiger, the isthmus of Panama, presents the three variables of tropical climates Af (tropical rainforest), Am (Monsoon), and Aw (dry winter savannah) [34]. Moreover, it is important to emphasize that some sectors of the Central Mountain Range represent climate C (mesothermal), and that the tropical precipitations in the Atlantic slope surpass 4000 mm, while in the Pacific

slope, the ranges extend from approximately 1000 to 3500 mm. Consequently, of the 37 life zones that have been proposed worldwide [35], as a result of the geomorphological and climatic contrast of the isthmus, Panama has 12 life zones classified into 3 types of humid forests, 4 of very humid forests, 3 of rainforests, and 2 of dry forests [36–38].

According to Köppen’s methodology [37], it is unquestionable that the research site evolved within a tropical climatic region with dry winter (Aw). It should be noted that the ombrothermal diagram (Figure 2) shows the existence of a dry period, since monthly rainfall does not reach 60 mm per month. Therefore, to determine the type of climatic region, the annual effect of aridity is delimited; applying Martonne’s index, $Im = (P \text{ mm}) / (T \text{ } ^\circ\text{C} + 10)$, $1725.2 / (27.6 + 10) = 45.8$, proves the existence of a humid climatic region, where Im has values >30 . This region is located in the Central American Dry Corridor, which climatically tends to have periodic droughts [39].

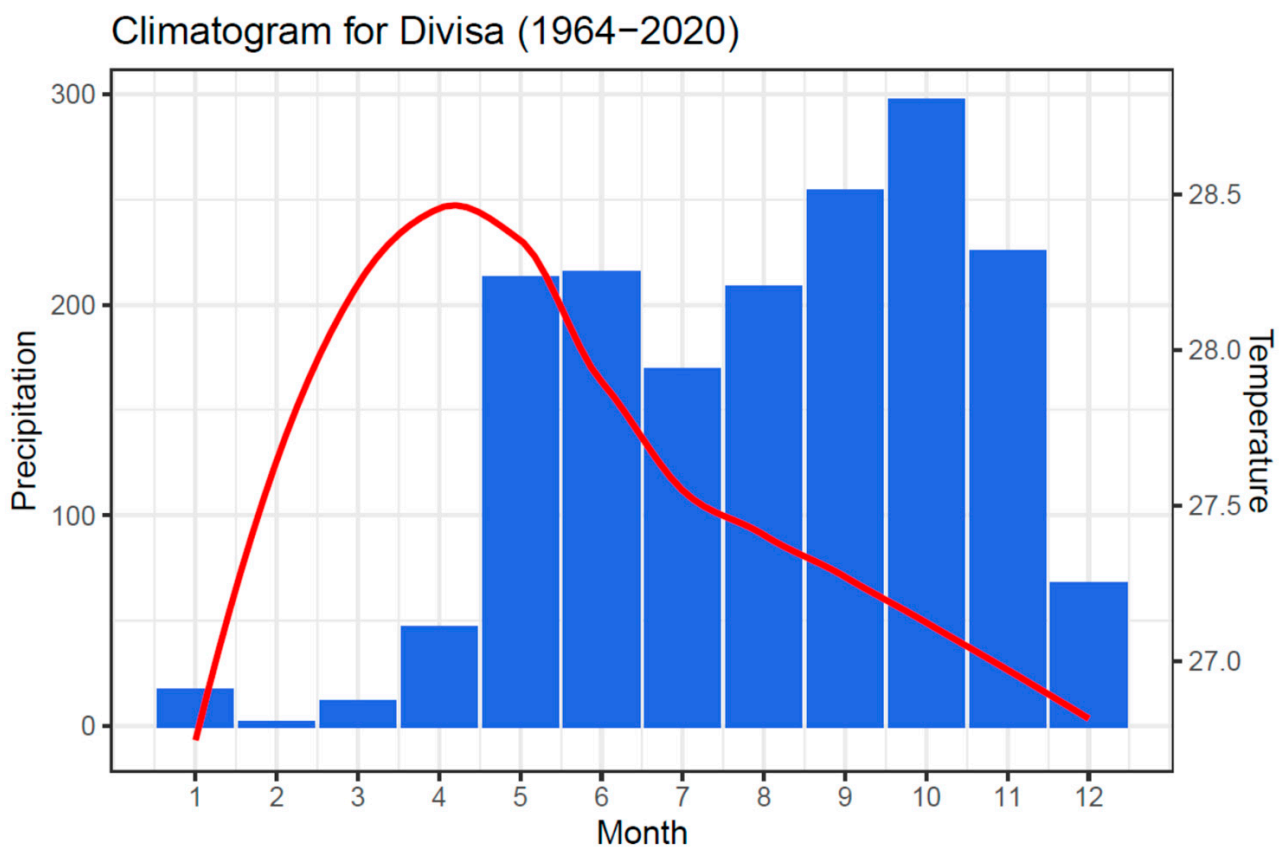


Figure 2. Climatogram of Divisa for the period 1964–2020. The red line represents mean monthly temperature, the blue line means monthly precipitation totals.

The chosen study area represents a unique karstic area located within the marine–coastal fringe in the the Ciénega de El Mangle wildlife refuge in Panama. It covers an area of 0.6531 ha (6531 m²), of which only 296.4 m² (296.4 m²) is covered by vegetation cover.

2.2. Geomorphological Mapping

Although detailed landscape and geomorphological mapping are useful tools for land use and disaster risk planning, such efforts in Central America are very scarce [40–45]. Therefore, geomorphological mapping presents a very important part of this study, which gives insight into the geomorphological characteristics of the studied karstic area. A geomorphological map of the study area was created following the recommendations for geomorphological mapping and terrain analysis given by Tricart [46] and Van Zuidam [47].

In order to identify and detect the karst research site and visualize the geomorphological features within the coastal strip, geoprocessing techniques were applied to the SRTM digital elevation model (DEM), in the ArcGIS 10.7.1 environment (ArcToolbox—Surface—Hillshade; and Slope). Next, the hypsometric criteria of the Instituto de Pesquisas Tecnológicas (Brazil) were applied to determine the type of relief [48] and elaborate the area that integrates the studied geosystem. Carried spatial analysis allowed the identification of drainage flows, water bodies, and the morphogenetic discrimination of the coastal marine geofacies that circumscribe the research site [49]. Moreover, we identify the particular presumably karstic depressions in the study area. Consequently, Topographic Sheets Mosaic for Panama was used as a reference for visual registration, comparison, and documentation of the landscape components within the study area (2012, Scale 1:25,000). Subsequently, in order to inventory the geofacies that make up the geosystem, natural landscape units were verified in the field [49], while the CNES/Airbus 2021 Image (Google Earth Pro) was used for additional verification. We will provide a comprehensive explanation of our detailed-scale identification process, encompassing fieldwork techniques and advanced technologies for discriminating various types of karstic depressions.

2.3. Karst Characterization and Analysis

Climatic data (temperature and precipitation) were acquired from the Divisa meteorological station understanding that the exposed geoforms are the product of a specific erosion system determined by the climate [50]. An important part of the work related to the karst characterization and analysis was fieldwork, which covered the following activities that were conducted in the field: (a) discrimination and documentation of natural landscapes according to the morphogenetic unit; (b) determination of the depth, alkalinity and texture of the soil (within one (1) trial pit cut); (c) use of global navigation satellite system (GNSS) for collection of the database (points) representing the identified geotopes (thus allowing the delimitation of different geofacies); (d) rock sampling within chosen geofacies and geotopes; (e) collection of morphometric and anatomical data for different geotopes; and (f) water sampling. The main aim of water sampling was the characterization of the origin of the water confined in the geotopes in order to determine their genesis. Water sampling was performed two times, in the rainy period of 2020 and the dry period of 2021, using the multi-parametric sensor, which is suitable for both fresh and salt water. The following parameters were measured with the multi-parametric sensor following the methodology suggested by the Standard Methods for the Examination of Water and Wastewater [51]: pH, temperature, salinity, conductivity, dissolved oxygen, turbidity, and alkalinity.

The second part of the work is related to the karst characterization and analysis covered activities carried out in the laboratory, where firstly collected rock samples (hand-held) were subjected to the following physical tests: (a) crushing and sieving (to segregate clasts and obtain a solute); (b) simple random sampling by magnetized capture of clasts retained in mesh (to determine the existence of ferromagnetic metals); (c) fissility testing (to check for parallel fracture of the stratification planes); (d) chemical testing of empirical solutions, used to demonstrate solubility with effervescence in acid (HCl) at ambient temperature using saturated samples of 1 g of pulverized rock (solute) diluted in 30 drops of HCl (1.5 mL) (solvent or solvent) and 1 clast of rock (solute) diluted in 3 drops of HCl (solvent).

Furthermore, collected water samples were also analyzed in the laboratory, where the following parameters were evaluated directly in each sump (containing water): pH, temperature, salinity, conductivity, total dissolved solids, dissolved oxygen, and turbidity. Water samples were taken from four sinkholes during the dry period in polypropylene bottles of 1 L capacity for each of the analyses of alkalinity, chloride concentrations, and hardness, which were placed in a cooler at 4 °C to demonstrate the amount of calcium carbonate present (CaCO₃), chlorides and calcium, respectively, using a volumetric method with colorimetric indicators.

Sulfate (SO_4) (mg/L) and iron (Fe^{3+}) (mg/L) were analyzed using the HACH model 850 photometer colorimeter equipment. Samples were also taken for bacteriological analysis in sterile 100-milliliter (mL) containers for the analysis of coliforms, *E. coli*, and Enterobacteriaceae using the Colilert technique (defined substrate) and hydrogen sulfide strips. The methodology used for the physicochemical and bacteriological analyses is based on the methods standardized by the Standard Methods for the Examination of Water and Wastewater [51]. The results of the soil and water samples are then compiled and interpreted, and the results of the physical and chemical tests applied to the rocks are compared to classify them.

3. Results and Discussion

3.1. Landforms and Processes within the Ciénega de El Mangle

A detailed geomorphological map, which was created based on a combination of terrain analysis and satellite imagery interpretation within the GIS environment, has been additionally verified by a field survey. As a result, the created geomorphological map has allowed localization of the study area within the marine–coastal fringe. The study area is located at ± 848 m from the perimeter that circumscribes the existence of a coastal lagoon (Figure 3). Consequently, the area that circumscribes the geosystem and exposes its geofacies was constructed (Figure 4), where the existence of a fluvial–marine plain that harbors mangroves stands out.

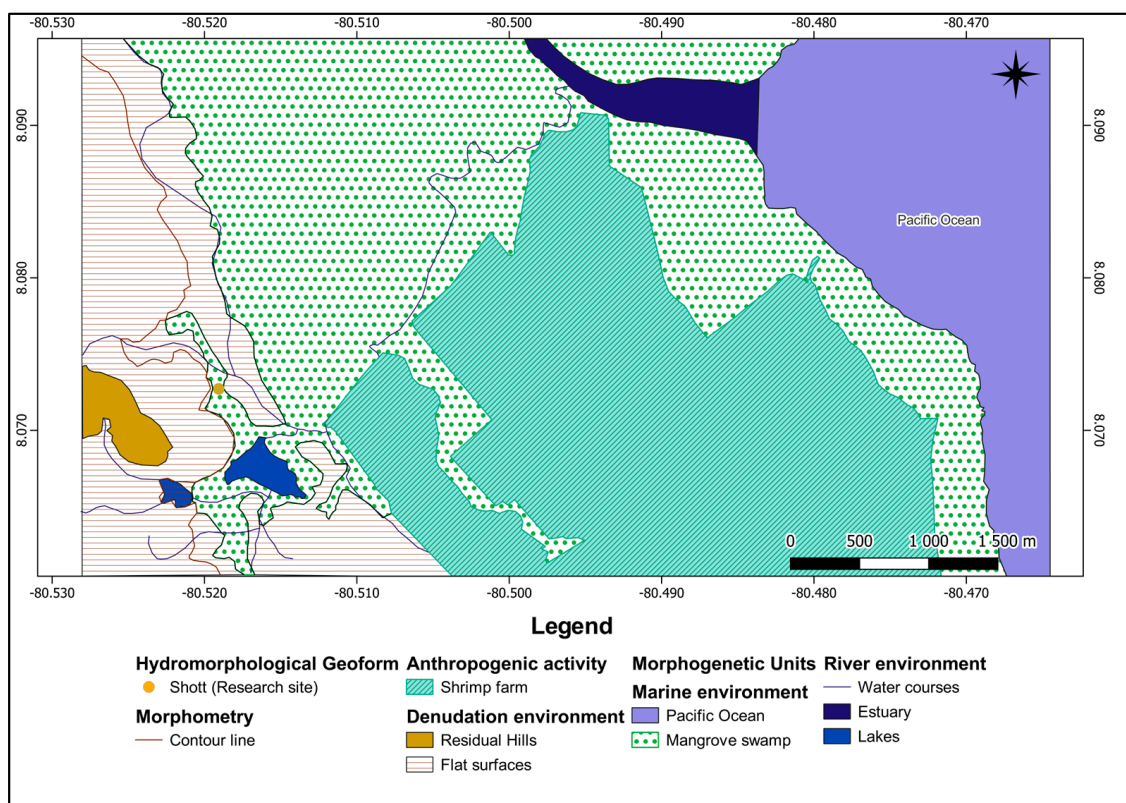


Figure 3. Geomorphological map of Ciénega de El Mangle, Panama.

Through the field survey that included the verification of mapped geomorphological geofacies and their geotopes, it was possible to identify different morphogenetic processes that have influenced the evolution of the study area. While the first process is related to the effects of efflorescence, which facilitated the classification of the geofacies (Figure 5), the second is related to the process of rock dissolution (Figure 6), which is an indispensable factor for the evolution of geofoms identified by sampling site (ID/1-2-3-4).

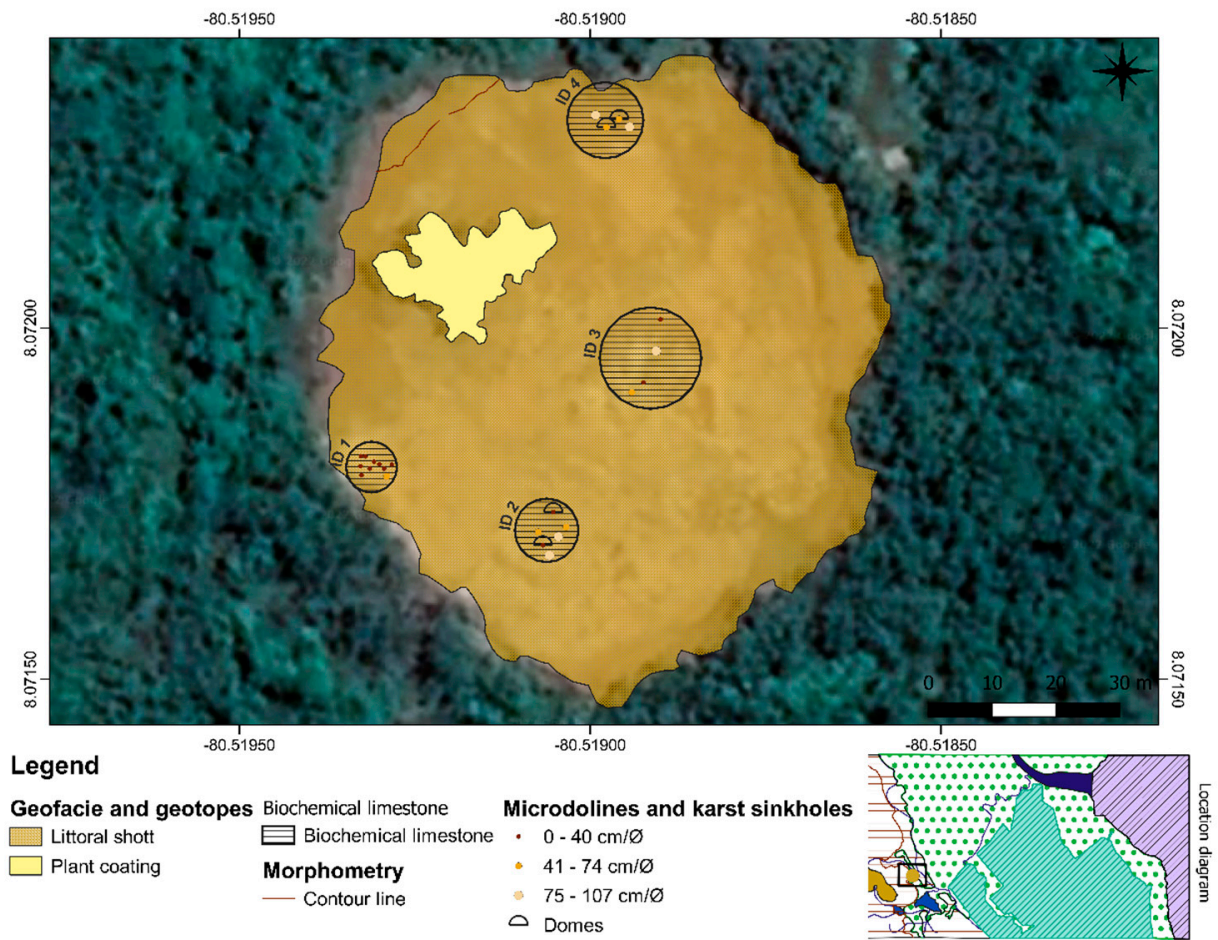


Figure 4. Geofacies and geotopes of Ciénega El Mangle, Panama.

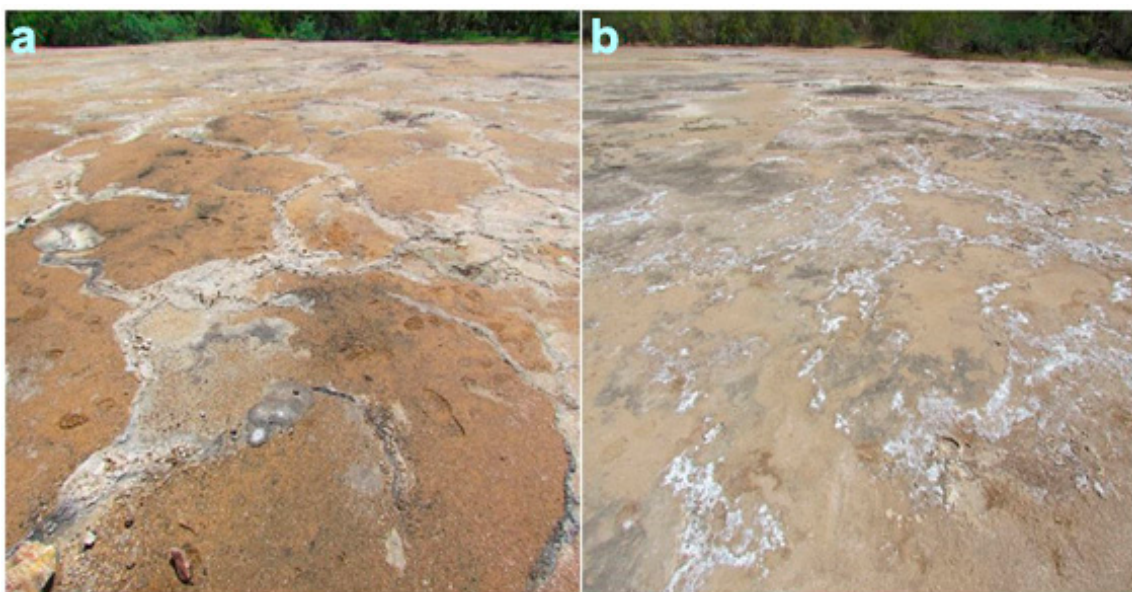


Figure 5. Littoral shott. (a) Partial view in rainy period showing a polygonal beach defined by calcareous crusts. (b) Partial view in dry period exposing the polygonal beach covered by salt precipitates (efflorescence), product of intense evaporation.



Figure 6. Karst sinkholes filled with brackish water and microdolines. (a) Micro-dolines filled of water during rainy season, the diameters are below half meter in most of them. (b–c) Saline efflorescence in micro-dolines. (d) Karst sinkholes over a meter diameter filled with water during dry season.

The interaction of marine and fluvial environments has led to the formation of a lagoon, a coastal marine geofacies that forms a transitional landscape between the ocean and coastal wetlands (Figure 4). From a geomorphological point of view, lagoons evolve parallel to the coastline, separated from the sea by shoals [51]. Since lagoons represent mixed water bodies formed by the interaction of fluvial and marine processes, their evolution is conditioned by the contribution of rainwater and fluvial waters, as well as saltwater intrusion (marine groundwater), and/or by ascent of saltwater through estuarine fluvial channels [52]. Large parts of the coastal area are covered by coastal wetlands, consisting mainly of mangrove swamps. Additionally, shrimp farms have replaced large parts of former mangrove swamps, a common problem in Central America and tropical regions [53,54].

The spatial analysis identified three types of morphogenetic environments responsible for the configuration and evolution of the detected geofacies and their geotopes. Thus, the circumscribed research area shows the incidence of the following three morphogenetic processes (landscape physiology): saline efflorescence, chemical weathering of rocks by dissolution, and physical weathering by haloclastism. These morphogenetic processes are responsible for the alkalinity of the soils and the reduction in vegetation cover, the genesis of in situ karst (landscape anatomy), and the evolution of the littoral shott (hydromorphological geoform).

The denudation environment influenced the formation of a peneplain on which the coastal and fluvial–marine plains are located, made up of flattened surfaces and residual hills, resulting from the prolonged weathering processes [9]. Carried soil analysis has confirmed the lacustrine origin of the deposits, while it was possible to determine the water table at a depth of 1.20 m. These deposits are the product of geomorphological-climatic processes [55]. These kinds of sediments are characterized by the predominance of silts and clays. The first horizon, in general, has a high organic matter content, and that the water table is located at an average depth of ± 2 m. Detected morphogenetic processes have led to the formation of littoral shott, which represents the most important feature of these geofacies.

Littoral shott represents a surface and/or ephemeral lake of varied sizes that reveal and show a saline film or substrate on the surface, generally associated with arid climates and intense evaporation [25]. Due to the fact that these landscapes also often occur in seasonal humid tropical climates, reflecting the high rate of evaporation during the dry period [52]. The term littoral is added to emphasize the location of the shott, which is located within the marine–coastal fringe, and to imply that the evolution of this geofacies is conditioned by the intrusion of marine water. The shott is part of the geofacies of hydromorphological origin, and it refers to a geofacies—plain or saline beach with groundwater supply, which, also arise when groundwater near the surface evaporates [56]. For the karst model development, it is necessary to have soluble fissured rocks on the surface or close to it, which gradually facilitates the passage of water [4]. In addition, the geosystem must receive a high volume of precipitation, which together with the surrounding vegetation intensifies the effects of the dissolution of the rock, since the concentration of CO₂ in the soil can be up to fifteen times greater than that in the atmosphere [57].

While during the rainy season, the littoral shott exposes a polygonal beach defined by overhanging calcareous crusts (Figure 5a), during the dry season, it exposes the polygonal beach covered by salt precipitates (efflorescence), a product of intense evaporation (Figure 5b; Table 1). It should be noted that in the geosystem that encloses the research site, this landscape unit is used for commercial purposes for the development of shrimp farms. In addition, adjacent to the perimeter that circumscribes the lagoon are the halomorphic soils, typical of the fluvial–marine plains on which mangrove forest develops.

Table 1. Morphometric characteristics of the geotopes formed by dissolution and haloclasticity, according to sampling site (ID). + is located where the value was present.

Site 1. Diameter 7 m.					
Totals ID	Diameter (cm)	Depth (cm)	Microdolines	Brackish-Water Karst Sinkhole	Exposed Domal Form: Average Height (cm)
1	40	21	+		
2	23	6	+		
3	38	13	+	+	
4	19	6	+	+	
5	22	6	+		
6	34	13	+		
7	20	13	+	+	
8	40	15	+		
9	49	20	+		
10	32	6	+		
Site 2. Diameter 10 m					
1	75	14	+		
2	38	12	+		14
3	107	5	+		
4	49	18	+		
5	48	8	+		
6	24	18	+		14
Site 3. Diameter 16 m					
1	42	11	+	+	
2	33	14	+	+	
3	105	15	+	+	
4	21	21	+	+	
Site 4. Diameter 10 m					
1	75	52	+		16
2	54	63	+		16
3	51	51	+		16
4	87	33	+		16

The soils of the research site may be showing the effects of iron chlorosis (very alkaline), evolving from a seasonal humid climate, biochemical limestone and conchiferous rocks, and seawater intrusion. In these soils the exchange complex is saturated, and the excess of calcium in the medium prevents other elements, such as iron, from being absorbed by plants. Therefore, in soils with $\text{pH} > 8$, (considered very alkaline), plants have difficulty growing because of the decrease in iron necessary for leaf development [58]. Evidently, efflorescence is the concentration of salts (sodium chloride, calcium, magnesium, and sodium sulfates) on the soil surface, as a result of evaporation, during the dry period in some landscapes of seasonally humid tropical climates and arid climates [59].

In the classification of geofacies and geotopes, the term karst is used to designate areas or geofoms whose structures are made up of carbonate rocks, which are characterized by specific genesis, which is mostly related to the gradual dissolution of the carbonate bedrock [4,60]. Although the studied karstic area is relatively small, covering only 6531 m², it represents a unique karstic environment that hosts several interesting karstic micro-forms that were formed by complex processes. As the studied karstic area is located within the marine–coastal fringe, it is influenced by a combination of different factors and processes. A humid climate and abundance of precipitation enhance the dissolution and weathering of carbonates, which is enhanced by the occasional influx of brackish groundwater, while on the other hand, high temperatures and intense evaporation promote the surficial deposition of evaporates.

Among the most common geofoms are various karstic depressions, which are part of the superficial karst landscapes, called exokarsts [4,61,62]. Such closed karstic depressions of different shapes and sizes that mostly appear where the underlying rock is soluble are often called dolines [4,57,63,64]. However, several other terms are present in the karst literature which consider different genesis or morphometric characteristics (size and depth) of such karstic depressions. Identification and characterization are especially complex for various small-scale karstic micro-features, which are often known as microkarren and karren [4,61,65].

Such small karstic forms that are made by surficial dissolution on bare or lightly vegetated carbonate rocks are also known as solution pits or, in the case of larger diameters, solution pans [4,65–68]. Although solution pans are documented in some tropical parts of Central America, such as the currently submerged solution pans of the Yucatán Peninsula [69], these terms have been rarely used in the scientific literature. The studied littoral shott hosts several shallow microdolines and sinkholes whose diameter is under 1 m, while depth is mainly under 0.5 m (Table 1). In total, 24 microdolines and sinkholes were identified within the four studied sites within the littoral shott, of which 6 represent domical geofoms resulting from evaporitic precipitation and 7 represent active karstic sinkholes filled with brackish water. The presence of brackish water in these seven karstic sinkholes is related to the influx of water through interconnected cracks in carbonate rocks.

The dissolution of evaporites is also responsible for the evolution of certain karstic micro-forms that are present within the studied littoral shott. These include several domical micro-forms that are present within two studied sites (2 and 4) within the littoral shott (Figure 6d). The diameter of these domical micro-forms ranges from 24 up to 87 cm, the depth ranges between 12 and 63 cm, and the height is significantly lower, ranging between 14 and 16 cm. While two domical micro-forms that were detected within site 2 have smaller diameters, heights and especially depths, four domical micro-forms located within site 4 have considerably larger diameters and depths, with slightly higher heights (Table 1). It is not uncommon that in areas with the presence of evaporites (salts), superficial and subsurface karst dissolution can cause the formation of various closed depressions [56]. The morphology of these domical micro-forms corresponds to the karstic salt domes found in the arid and semiarid parts of the world, which are known for intense evaporation [70]. Furthermore, it should be noted that the finding of these karstic domical micro-forms corresponds to the results of other studies that were carried out in similar tropical coastal areas. The karstic modeling of the relief also develops in evaporites, generating on the

shott a varied superficial micro-form, whose formation is conditioned by the composition and depth of the groundwater [59]. These sometimes expose small domical forms, with diameters close to 1 m and 0.5 m high with an average depth of 20 cm. Several authors agree that the genesis of the domes is attributed to the dissolution and in situ precipitation of evaporites [56].

3.2. Karst Characteristics

The trial pit cut carried out at the perimeter of the research site during the dry period (March 2021) allowed verification of the existence of the deep soil (1.20 m), which can be divided into two main horizons: H1, with a depth of 0–5 cm, and H2, with a depth of 5–120 cm. Furthermore, it was possible to identify the water accumulated in the subsoil (water table), the equivalent point between the atmospheric pressure and the body of water (Figure 7). Table 2 shows the results of the granulometric analysis, pH, iron (Fe), calcium (Ca), and organic matter (OM), for each detected soil horizon.

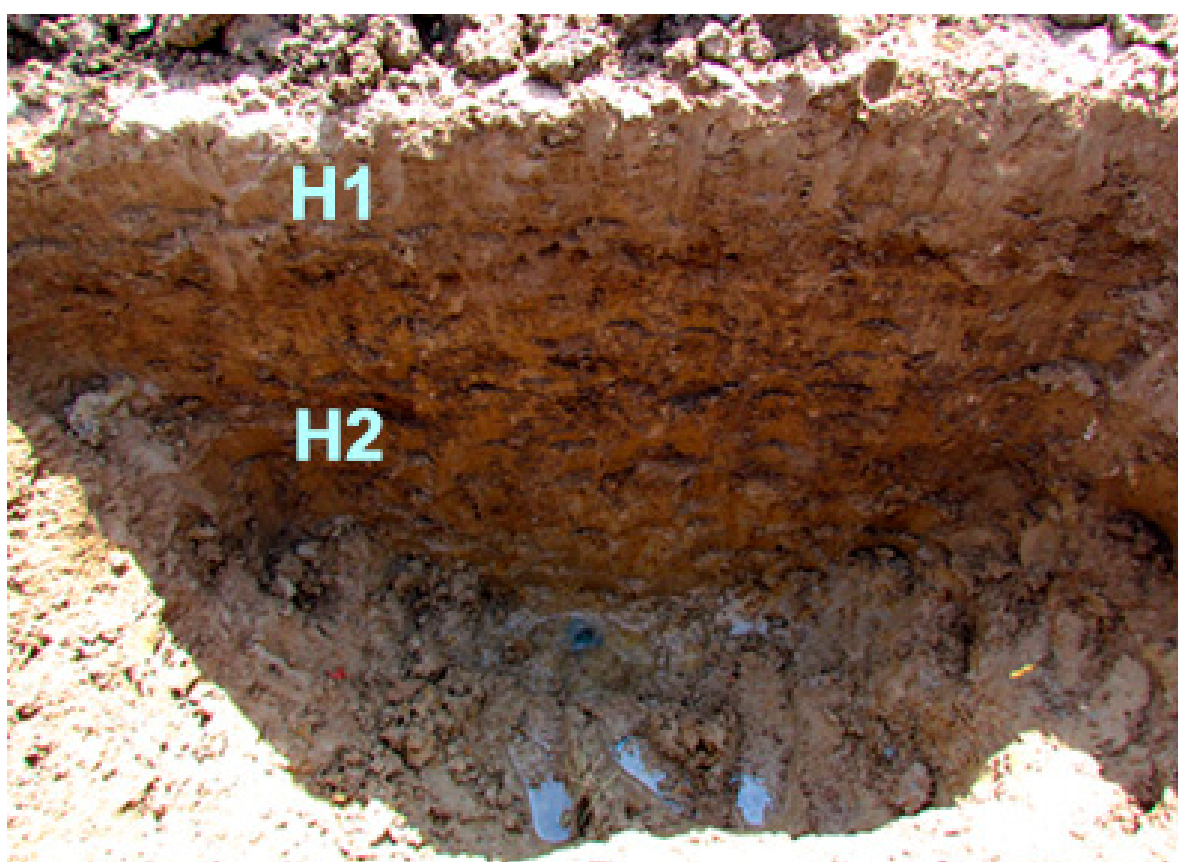


Figure 7. Trial pit of 1.2 m depth and two horizons (H1 and H2).

Table 2. Trial pit determination of soil textures, and basic chemical and biological characteristics. SOM: soil organic matter.

Horizon	Sand (%)	Silt (%)	Clay (%)	pH units	Ca (mg/L)	Fe (mg/L)	SOM (%)
1	68	16	16	8.5	85.4	0	79
2	32	18	50	8.1	149	29.1	0

During the field sampling, rock collection (hand samples) was carried out taking advantage of outcrops on the geofacies, and directly on the geotopes. The selected clast by simple random sampling (sieve 60) shows effervescence (seen through the stereomicroscope) before HCl at a certain time. Moreover, pulverized gram (bottom of sieve 230),

showed effervescence to HCl in time. In addition, rock outcrops on the geofacies showed remains of shells of marine organisms such as bivalves and gastropods, which confirms that carbonate rocks were formed within a paleo-marine environment (Figure 8).

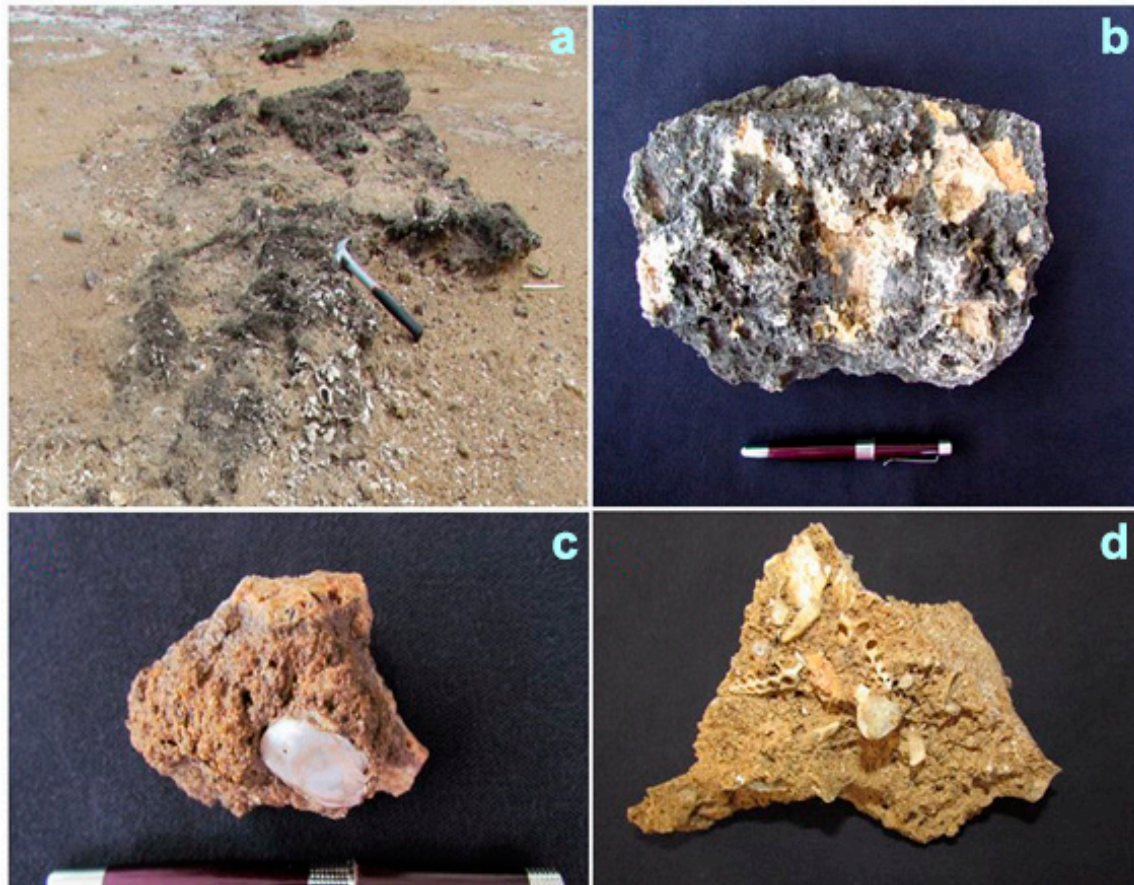


Figure 8. (a) Shelly limestone (coquina) rock outcrop on the geofacies, where remains of shells of marine organisms were observed. (b) Hand sample from the rock coquina outcrop. (c) Fractured hand sample on which bivalve shells are attached. (d) Fractured hand sample within which remains of bivalves and gastropods are embedded.

The lithological analysis of the warm and shallow waters of the tropical coasts presently represents the main unit of the landscape where the formation of large accumulations of coral reefs and shell beaches occurs. Therefore, in this natural space, various marine, chemical, and organic processes occur that end up facilitating the precipitation of carbonates, resulting in limestone beaches and reef limestones [71,72]. Among these are the conchiferous limestones, which are formed by the calcareous skeletal remains of marine fauna that inhabited the shallow waters along the coastline [59].

Consequently, the existence of conchiferous limestones—coquina (composed of CaCO_3 , of clastic texture with remains of shells and visible weakly cemented skeletons), constituted by organisms typical of the epifauna (bivalves and gastropods)—within our study area, about 5 km from the current coastline, is evidence of the effects of the last eustatic variation known as the Flandrian transgression [73–78]. This variation, which occurred approximately 20,000 years ago, produced an alteration to the water volumes of the oceans, modifying the marine–coastal strip of the Panamanian Pacific, until it stabilized about 6000 years ago. Within the Quaternary period, due to its fossiliferous content, the marine deposits of the Pleistocene and Holocene fauna are represented by the predominance of gastropods and epifaunal bivalves [79].

Water quality analysis aimed at the determination of the origin of the water within sinkholes was analyzed within two climatic extremes of the study site (rainy and dry periods). Water analysis of the four chosen sinkholes during the rainy season (October 2020) indicated a mean depth of 30 cm, the presence of coliforms, a mostly positive result for entire bacteria, a mean pH of 8.36, an average conductivity of 26.49 mS/cm, a mean dissolved oxygen of 4.82 mg/L, an average turbidity of 74.3 UNT, a mean temperature of 31 °C, an average alkalinity of 420.3 mg/L, a mean sulfate of 214.2 mg/L, a mean iron concentration of 0.23 mg/L, and an average PSU of 19.4. On the other hand, during the dry season (March 2021), two sinkholes were completely dry, while the other two indicated an average depth of 21 cm, presence of coliforms, a mostly positive result for entire bacteria, a mean pH of 7.17, an average conductivity of 17.62 mS/cm, a mean dissolved oxygen of 3.21 mg/L, an average turbidity of 52.5 UNT, a mean temperature of 28.3 °C, an average alkalinity of 622 mg/L, a mean sulfate of 1053.5 mg/L, a mean iron concentration of 378.5 mg/L, and an average PSU of 8.5.

In these water quality results of the sinkholes, the conductivity variable stands out, showing high values above 10,000 $\mu\text{S}/\text{cm}$, typical of brackish water of marine origin. Regarding pH values, the tendency of an alkaline pH was the main characteristic of the analyses. An important factor that influences the pH of marine waters is the solubility of CO_2 , which is mainly a function of salinity and temperature [59]. Moreover, sulfate, salinity, dissolved oxygen, and temperature values in the study site indicate water of marine origin. Tropical coastal environments can exhibit important spatial and temporal variations, reflecting changes in salinity, temperature, depth, turbulence, time of day, time of year, and biological activity [58].

Considering the results of the solubility tests with effervescence (HCl/ambient temperature) it is evident that sampled rocks represent biochemical rocks, constituted by calcium carbonate (CaCO_3), which in tropical climates evolves easily in shallow water coastal marine environments. These environments' calcite is derived mainly from marine organisms from calcium (Ca^{2+}) and bicarbonate (HCO_3^-) ions dissolved in seawater [59]. Consequently, due to the location and climatic characteristics of the research site, the geomorphological features are the result of the joint action of weathering processes (chemical and physical). On one hand, during the rainy season, the high rates of rainfall activate the dissolution process of the biogeochemical limestone rocks, since CaCO_3 shows high solubility in the presence of slightly acidic water, activating the diagenetic processes (dissolution, cementation, and replacement), as it percolates through the pores [59]. On the other hand, during the dry period, the geofacies present efflorescence (transforming it into a saline plain, also called littoral shott), where evaporation is the mechanism that triggers the precipitation of salts (CaCl_2). Among the mainly precipitated minerals in the marine-coastal fringes is halite (sodium chloride CaCl_2), composed mainly of rock salt. This condition is developed due to the fact that in the geological past many areas that are now drylands were coastal fringes submerged under shallow seas [56]. Moreover, in such environments, haloclastism is also responsible for the weathering of rocks [80]. This phenomenon is exacerbated by the alternation of dry and wet periods in seasonal climates [81]; therefore, the precipitation of these salts between the pores of the rock gives rise to volumetric expansions that produce disruptive stress that finally contributes to the disintegration of the rock [79,82].

4. Conclusions

The research site is a unique karstic area located within the marine-coastal fringe in the Ciénega de El Mangle wildlife refuge in Panama. As the research site is located on the periphery of the lagoon, it is affected by several interconnected processes, including seawater intrusion (through sinkholes), the formation of conchiferous limestone (CaCO_3), and NaCl precipitation via efflorescence. The morphoclimatic analysis indicates that it has a seasonally humid tropical climate, so chemical weathering processes are considered intense. Moreover, it contains less soluble alkaline soils, which hinders the development of vegetation.

The geomorphology of the area is the result of intense evaporation combined with the influx of brackish groundwater; landscapes evolve in the marine–coastal strips of seasonal tropical climates that exhibit saline beaches, called littoral shott. The shott encompasses various sinkholes formed by dissolution enhanced by saline intrusion. In addition, it exposes outcrops of carbonate sedimentary rocks (conchiferous limestones/ CaCO_3), and evaporites (common salt/ NaCl). These rock materials are susceptible to dissolution weathering and haloclastic weathering processes. Therefore, they constitute the sedimentary rock materials suitable for developing karst geoforms.

The karst cycle (susceptible to interruption at any stage) begins with the evolution of elemental geoforms such as sinkholes and microdolines, which represent evidence of an embryonic or juvenile karst. These geoforms evolve as a result of the correlation between sedimentary rock materials and the influence of surface and groundwater flows. The product is the formation of surface depressions due to the dissolution and physical disintegration of the rocks. In fact, the existence of these soluble rocks on the littoral shott facilitated the evolution of 24 sinkholes and microdolines, 6 of which show domical geoforms resulting from evaporitic precipitation and 7 of which represent active karstic sinkholes filled with brackish water.

Author Contributions: Conceptualization, J.R.-S.; methodology, J.R.-S.; software, J.R.-S.; validation, J.R.-S.; formal analysis, J.R.-S., A.Q.-R. and F.D.; investigation, J.R.-S., A.Q.-R. and F.D.; writing—original draft preparation, J.R.-S., A.Q.-R. and F.D.; writing—review and editing, J.R.-S., A.Q.-R. and F.D.; visualization, J.R.-S. and A.Q.-R.; supervision, A.Q.-R. All authors have read and agreed to the published version of the manuscript.

Funding: This research received no external funding.

Data Availability Statement: Data are available under request.

Acknowledgments: Hugo Rodríguez-Bolaños who assisted on several tasks during the research process and Soll Kracher for her English grammar syntax corrections.

Conflicts of Interest: The authors declare no conflict of interest.

References

1. Brunović, D.; Miko, S.; Ilijanić, N.; Peh, Z.; Hasan, O.; Kolar, T.; Razum, I. Holocene foraminiferal and geochemical records in the coastal karst dolines of Cres Island, Croatia. *Geol. Croat.* **2019**, *72*, 19–42. [[CrossRef](#)]
2. Benac, Č.; Juračić, M.; Matičec, D.; Ružić, I.; Pikelj, K. Fluviokarst and classical karst: Examples from the Dinarics (Krk Island, northern Adriatic, Croatia). *Geomorphology* **2013**, *184*, 64–73. [[CrossRef](#)]
3. Veress, M. Karst types and their karstification. *J. Earth Sci.* **2020**, *31*, 621–634. [[CrossRef](#)]
4. Ford, D.; Williams, P. *Karst Hydrogeology and Geomorphology*; John Wiley & Sons: Hoboken, NJ, USA, 2007.
5. Goldscheider, N.; Chen, Z.; Auler, A.S.; Bakalowicz, M.; Broda, S.; Drew, D.; Hartmann, J.; Jiang, G.; Moosdorf, N.; Stevanovic, Z.; et al. Global distribution of carbonate rocks and karst water resources. *Hydrogeol. J.* **2020**, *28*, 1661–1677. [[CrossRef](#)]
6. Quesada-Román, A.; Torres-Bernhard, L.; Ruiz-Álvarez, M.A.; Rodríguez-Maradiaga, M.; Velázquez-Espinoza, G.; Espinosa-Vega, C.; Toral, J.; Rodríguez-Bolaños, H. Geodiversity, Geoconservation, and Geotourism in Central America. *Land* **2022**, *11*, 48. [[CrossRef](#)]
7. Bauer-Gottwein, P.; Gondwe, B.R.; Charvet, G.; Marín, L.E.; Rebolledo-Vieyra, M.; Merediz-Alonso, G. The Yucatán Peninsula karst aquifer, Mexico. *Hydrogeol. J.* **2011**, *3*, 507–524. [[CrossRef](#)]
8. Aguilar, Y.; Bautista, F.; Mendoza, M.E.; Frausto, O.; Ihl, T. Density Of karst depressions in Yucatán state, Mexico. *J. Cave Karst Stud.* **2016**, *78*, 51–60. [[CrossRef](#)]
9. Marshall, J.S. The geomorphology and physiographic provinces of Central America. In *Central America: Geology, Resources and Hazards*; Taylor-Francis Group: Abingdon, UK, 2007; pp. 75–121.
10. Day, M. Karst landscapes. In *Central America: Geology, Resources and Hazards*; Bundschuc, J., Alvarado, G.E., Eds.; Taylor & Francis Group: Abingdon, UK, 2007; p. 1436.
11. Parise, M.; Gunn, J. Natural and anthropogenic hazards in karst areas: An introduction. *Geol. Soc. Lond. Spec. Publ.* **2007**, *279*, 1–3. [[CrossRef](#)]
12. De Waele, J.; Gutiérrez, F.; Parise, M.; Plan, L. Geomorphology and natural hazards in karst areas: A review. *Geomorphology* **2011**, *134*, 1–8. [[CrossRef](#)]

13. Gutiérrez, F.; Parise, M.; De Waele, J.; Jourde, H. A review on natural and human-induced geohazards and impacts in karst. *Earth Sci. Rev.* **2014**, *138*, 61–88. [[CrossRef](#)]
14. Xiong, K.; Yin, C.; Ji, H. Soil erosion and chemical weathering in a region with typical karst topography. *Environ. Earth Sci.* **2018**, *77*, 500. [[CrossRef](#)]
15. Domazetović, F.; Šiljeg, A.; Lončar, N.; Marić, I. Development of automated multicriteria GIS analysis of gully erosion susceptibility. *Appl. Geogr.* **2019**, *112*, 102083. [[CrossRef](#)]
16. Zhou, L.; Wang, X.; Wang, Z.; Zhang, X.; Chen, C.; Liu, H. The challenge of soil loss control and vegetation restoration in the karst area of southwestern China. *Int. Soil Water Conserv. Res.* **2020**, *8*, 26–34. [[CrossRef](#)]
17. Marín, A.I.; Francisco, M.R.J.; Barberá, J.A.; Fernández-Ortega, J.; Matías, M.; Damián, S.; Bartolomé, A. Groundwater vulnerability to pollution in karst aquifers, considering key challenges and considerations: Application to the Ubrique springs in southern Spain. *Hydrogeol. J.* **2021**, *29*, 379–396. [[CrossRef](#)]
18. Benito, G.; Sancho, C.; Peña, J.L.; Machado, M.J.; Rhodes, E.J. Large-scale karst subsidence and accelerated fluvial aggradation during MIS6 in NE Spain: Climatic and paleohydrological implications. *Quat. Sci. Rev.* **2010**, *29*, 2694–2704. [[CrossRef](#)]
19. Gutiérrez, F.; Benito-Calvo, A.; Carbonel, D.; Desir, G.; Sevil, J.; Guerrero, J.; Fabregat, I. Review on sinkhole monitoring and performance of remediation measures by high-precision leveling and terrestrial laser scanner in the salt karst of the Ebro Valley, Spain. *Eng. Geol.* **2019**, *248*, 283–308. [[CrossRef](#)]
20. Gijón-Yescas, G.; Aguilar-Duarte, Y.; Frausto-Martínez, O.; Bautista-Zuñiga, F. Anatomy of a cenote with use of dron. *Trop. Subtrop. Agroecosyst.* **2021**, *24*, 30. [[CrossRef](#)]
21. Fragoso-Servón, P.; Pereira Corona, A.; Bautista Zúñiga, F.; Prezas Hernández, B.; Reyes, N.A. Soils in extreme conditions: The case of the catenas karst-marsh-coastline in the Mexican Caribbean. *Boletín Soc. Geológica Mex.* **2020**, *72*, A040619. [[CrossRef](#)]
22. Rodríguez-Castillo, J.F.; Frausto-Martínez, O.; Uhu-Yam, W.D.; Colín-Olivares, O. Caracterización morfológica de depresiones kársticas: Zona costera nororiente de la Península de Yucatán, México. *Ecosistemas Recur. Agropecu.* **2022**, *9*. [[CrossRef](#)]
23. Day, M. Challenges to sustainability in the Caribbean karst. *Geol. Croat.* **2010**, *63*, 149–154. [[CrossRef](#)]
24. Day, M. Protection of karst landscapes in the developing world: Lessons from Central America, the Caribbean, and Southeast Asia. In *Karst Management*; Springer: Berlin/Heidelberg, Germany, 2011; pp. 439–458.
25. Lace, M.J. Advances in the Exploration and Management of Coastal Karst in the Caribbean. In *Environmental Management and Governance: Advances in Coastal and Marine Resources*; Springer International Publishing: Berlin/Heidelberg, Germany, 2014; pp. 143–172.
26. Klaas, D.K.; Imteaz, M.A.; Sudiayem, I.; Klaas, E.M.; Klaas, E.C. Assessing climate changes impacts on tropical karst catchment: Implications on groundwater resource sustainability and management strategies. *J. Hydrol.* **2020**, *582*, 124426. [[CrossRef](#)]
27. Rockwell, T.K.; Bennett, R.A.; Gath, E.; Franceschi, P. Unhinging an indenter: A new tectonic model for the internal deformation of Panama. *Tectonics* **2010**, *29*. [[CrossRef](#)]
28. Alvarado, G.E.; Benito, B.; Staller, A.; Climent, Á.; Camacho, E.; Rojas, W.; Lindholm, C. The new Central American seismic hazard zonation: Mutual consensus based on up to day seismotectonic framework. *Tectonophysics* **2017**, *721*, 462–476. [[CrossRef](#)]
29. Harmon, R. *The Chagres River, Panama: A Multidisciplinary Profile of a Tropical Watershed*; Kluwer Academic Publishers: Boston, MA, USA; Dordrecht, The Netherlands; London, UK, 2005.
30. Montes, C.; Hoyos, N. Isthmian bedrock geology: Tilted, bent, and broken. In *The Geology of Colombia, Paleogene–Neogene. Servicio Geológico Colombiano*; Gómez, J., Mateus-Zabala, D., Eds.; Publicaciones Geológicas Especiales: Bogotá, Colombia, 2020; Volume 3, pp. 451–467.
31. Bacon, C.; Molnar, P.; Antonelli, A.; Crawford, A.; Montes, C.; Vallejo-Pareja, M. Quaternary glaciation and the Great American Biotic Interchange. *Geology* **2016**, *44*, 375–378. [[CrossRef](#)]
32. Palka, E. A geographical view of Panama. In *The Río Chagres, Panama*; Harmon, R.S., Ed.; Library of Water Science and Technology; Springer: Dordrecht, The Netherlands, 2005; Volume 52.
33. Quesada-Román, A.; Ballesteros-Cánovas, J.A.; Guillet, S.; Madrigal-González, J.; Stoffel, M. Neotropical *Hypericum irazuense* shrubs reveal recent ENSO variability in Costa Rican páramo. *Dendrochronologia* **2020**, *61*, 125704. [[CrossRef](#)]
34. Madrigal-González, J.; Calatayud, J.; Ballesteros-Cánovas, J.A.; Escudero, A.; Cayuela, L.; Rueda, M.; Ruiz-Benito, P.; Herrero, A.; Aponte, C.; Sagardia, R.; et al. Climate reverses directionality in the richness–abundance relationship across the World’s main forest biomes. *Nat. Commun.* **2020**, *11*, 5635. [[CrossRef](#)] [[PubMed](#)]
35. Grossman, E.; Robbins, J.; Rachello-Dolmen, P.; Tao, K.; Saxena, D.; O’Dea, A. Freshwater input, upwelling, and the evolution of Caribbean coastal ecosystems during formation of the Isthmus of Panama. *Geology* **2019**, *47*, 857–861. [[CrossRef](#)]
36. National Geographic Institute “Tommy Guardia”. *National Atlas of the Republic of Panama Colombia*, 5th ed.; Impresiones Carpal: Panama, Colombia, 2016.
37. Peel, M.C.; Finlayson, B.; McMahon, T. Updated world map of the Köppen-Geiger climate classification. *Hydrol. Earth Syst. Sci.* **2007**, *11*, 1633–1644. [[CrossRef](#)]
38. Holdridge, L. *Life Zone Ecology. Inter-American Institute for Cooperation on Agriculture*, 4th ed.; Tropical Science Center: San José, Costa Rica, 1996.
39. Quesada-Hernandez, L.E.; Calvo-Solano, O.D.; Hidalgo, H.G.; Perez-Briceno, P.M.; Alfaro, E.J. Dynamical delimitation of the Central American Dry Corridor (CADC) using drought indices and aridity values. *Prog. Phys. Geogr. Earth Environ.* **2019**, *43*, 627–642. [[CrossRef](#)]

40. Quesada-Román, A.; Mata-Cambronero, E. The geomorphic landscape of the Barva volcano, Costa Rica. *Phys. Geogr.* **2021**, *42*, 265–282. [[CrossRef](#)]
41. Quesada-Román, A.; Castro-Chacón, J.P.; Boraschi, S.F. Geomorphology, land use, and environmental impacts in a densely populated urban catchment of Costa Rica. *J. S. Am. Earth Sci.* **2021**, *112*, 103560. [[CrossRef](#)]
42. Quesada-Román, A. Geomorphology of the Guacimal River catchment, Costa Rica. *J. Geogr. Cartogr.* **2022**, *5*, 58–67. [[CrossRef](#)]
43. Quesada-Román, A.; Quirós-Arias, L.; Zamora-Pereira, J.C. Interactions between Geomorphology and Production Chain of High-Quality Coffee in Costa Rica. *Sustainability* **2022**, *14*, 5265. [[CrossRef](#)]
44. Quesada-Román, A.; Peralta-Reyes, M. Geomorphological Mapping Global Trends and Applications. *Geographies* **2023**, *3*, 610–621. [[CrossRef](#)]
45. Quesada-Román, A.; Umaña-Ortíz, J.; Zumbado-Solano, M.; Islam, A.; Abioui, M.; Tefogoum, G.Z.; Kariminejad, N.; Mutaqin, B.W.; Pupim, F. Geomorphological regional mapping for environmental planning in developing countries. *Environ. Dev.* **2023**, *48*, 100935. [[CrossRef](#)]
46. Tricart, J. Cartographie géomorphologique. *Ann. Géograph.* **1972**, *81*, 751–753.
47. Van Zuidam, R. *Aerial Photo-Interpretation in Terrain Analysis and Geomorphologic Mapping*; Smits Publishers: Cherry Hill, NJ, USA, 1986; p. 25102.
48. Tamiozzo, F.; Marques, R.; De Oliveira, S. *Introdução à Geomorfologia*; Cengage Learning: Boston, MA, USA, 2013.
49. Espinosa-Pérez, I.D.; García-Romero, A.; Cruz-Fuentes, L.F. Proposal of Differentiating Components for the Multiscale Classification of the Landscape. *Investig. Geográficas* **2022**, *107*, e60539.
50. Rivera-Solís, J.A. Depósitos eólicos del trópico húmedo: Caso de la franja marino-costera del este de la Península de Azuero, Panamá. *Rev. Geográfica América Cent.* **2021**, *66*, 79–105. [[CrossRef](#)]
51. Wef, A.A. *Standard Methods for the Examination of Water and Wastewater*; American Public Health Association, American Water Works Association, Water Environment Federation: Washington, DC, USA, 2005.
52. Bird, E.C. *Physical Setting and Geomorphology of Coastal Lagoons*; Elsevier Oceanography Series; Elsevier: Amsterdam, The Netherlands, 1994; Volume 60, pp. 9–39.
53. Medina-Gómez, I.; Kjerfve, B.; Mariño, I.; Herrera-Silveira, J. Sources of salinity variation in a coastal lagoon in a karst landscape. *Estuaries Coasts* **2014**, *37*, 1329–1342. [[CrossRef](#)]
54. Acuña-Piedra, J.F.; Quesada-Román, A. Multidecadal biogeomorphic dynamics of a deltaic mangrove forest in Costa Rica. *Ocean. Coast. Manag.* **2021**, *211*, 105770. [[CrossRef](#)]
55. Veas-Ayala, N.; Alfaro-Córdoba, M.; Quesada-Román, A. Costa Rican wetlands vulnerability index. *Prog. Phys. Geogr. Earth Environ.* **2023**, *47*, 521–540. [[CrossRef](#)]
56. Zinck, J.A. *Geopedology, Elements of Geomorphology for Soil and Geohazard Studies*; ITC Special Lecture Notes Series; ITC Faculty of Geo-Information Science and Earth Observation: Enschede, The Netherlands, 2013.
57. Goudie, A. (Ed.) *Encyclopedia of Geomorphology*; Psychology Press: London, UK, 2004; Volume 2.
58. Mees, F.; Tursina, T.V. Salt minerals in saline soils and salt crusts. In *Interpretation of Micromorphological Features of Soils and Regoliths*; Elsevier: Amsterdam, The Netherlands, 2018; pp. 289–321.
59. Buol, S.W.; Southard, R.J.; Graham, R.C.; McDaniel, P.A. *Soil Genesis and Classification*; John Wiley & Sons: Hoboken, NJ, USA, 2011.
60. Durand, N.; Monger, H.C.; Canti, M.G.; Verrecchia, E.P. Calcium carbonate features. In *Interpretation of Micromorphological Features of Soils and Regoliths*; Elsevier: Amsterdam, The Netherlands, 2018; pp. 205–258.
61. Veress, M. Factors influencing solution in karren and on covered karst. *Hung. Geogr. Bull.* **2010**, *59*, 289–306.
62. Waltham, A.C.; Fookes, P.G. Engineering classification of karst ground conditions. *Q. J. Eng. Geol. Hydrogeol.* **2003**, *36*, 101–118. [[CrossRef](#)]
63. Jourde, H.; Wang, X. Advances, challenges and perspective in modelling the functioning of karst systems: A review. *Environ. Earth Sci.* **2023**, *82*, 396. [[CrossRef](#)]
64. Monroe, W.H. *A Glossary of Karst Terminology*; U.S. Government Printing Office: Washington, DC, USA, 1970.
65. Jennings, J.N. Cave and karst terminology. *Aust. Karst Index* **1985**, 1–13.
66. Perica, D.; Marjanac, T.; Aničić, B.; Mrak, I.; Juračić, M. Small karst features (karren) of Dugi Otok island and Kornati archipelago coastal karst (Croatia). *Acta Carsologica* **2004**, *33*. [[CrossRef](#)]
67. Taboroši, D.; Jenson, J.W.; Mylroie, J.E. Karren features in island karst: Guam, Mariana Islands. *Z. Geomorphol.* **2004**, *48*, 369–389. [[CrossRef](#)]
68. Ginés, A.; Knez, M.; Slabe, T.; Dreybrodt, W. (Eds.) *Karst Rock Features. Karren Sculpturing: Karren Sculpturing*; Založba ZRC: Ljubljana, Slovenia, 2009; Volume 9.
69. Knez, M.; Rubinić, J.; Slabe, T.; Šegina, E. Karren of the Kamenjak Hum (Dalmatian Karst, Croatia); from the initial dissection of flat surfaces by rain to rocky points. *Acta Carsologica* **2015**, *44*. [[CrossRef](#)]
70. Goff, J.A.; Gulick, S.P.; Cruz, L.P.; Stewart, H.A.; Davis, M.; Duncan, D.; Fucugauchi, J.U. Solution pans and linear sand bedforms on the bare-rock limestone shelf of the Campeche Bank, Yucatán Peninsula, Mexico. *Cont. Shelf Res.* **2016**, *117*, 57–66. [[CrossRef](#)]
71. Jennings, J.N. The disregarded karst of the arid and semiarid domain/Le karst méconnu du domaine aride et semi-aride. *Karstologia* **1983**, *1*, 61–73. [[CrossRef](#)]
72. Soja, C.M. Island-arc carbonates: Characterization and recognition in the ancient geologic record. *Earth Sci. Rev.* **1996**, *41*, 31–65. [[CrossRef](#)]

73. Castanier, S.; Le Métayer-Levrel, G.; Perthuisot, J.P. Ca-carbonates precipitation and limestone genesis—The microbiogeologist point of view. *Sediment. Geol.* **1999**, *126*, 9–23. [[CrossRef](#)]
74. Rivera, J.A. Análisis geomorfológico de la región costera del este “E”, de la provincia de Los Santos. *Rev. Geográfica América Cent.* **2011**, *2*, 1–14.
75. Rivera, J.A. Propuesta de zonificación ambiental del paisaje marino costero: Cuenca del Río Purio. *Visión Antataura* **2017**, *1*, 93–94.
76. Quesada-Román, A.; Pérez-Briceño, P.M. Geomorphology of the Caribbean coast of Costa Rica. *J. Maps* **2019**, *15*, 363–371. [[CrossRef](#)]
77. Rivera-Solis, J.A. Estudio Geomorfológico para la Ordenación del Espacio Litoral: Caso del Estuario del Río Purio, República de Panamá. *Investig. Geográficas* **2016**, *52*, 83–98. [[CrossRef](#)]
78. Rivera-Solis, J.A.; Cortez, A.T.C. Classificação das paisagens da faixa marinha costeira da bacia hidrográfica do Rio Purio, República do Panamá. *Estud. Geogr. Rev. Eletron. Geogr.* **2015**, *13*, 77–93.
79. Rivera-Solis, J.A. *Teoría y Métodos para la Práctica de la Geografía Física: Estudios de Casos—Panamá*; Editora Novo Art S.A.: Panamá, Colombia, 2016; p. 176.
80. Charó, M.; Fucks, E.; Gordillo, S. Moluscos marinos bentónicos del Cuaternario de Bahía Anegada (sur de Buenos Aires, Argentina): Variaciones faunísticas en el Pleistoceno tardío y Holoceno. *Rev. Mex. Cienc. Geol.* **2013**, *30*, 404–416.
81. Willgoose, G. *Principles of Soilscape and Landscape Evolution*; Cambridge University Press: Cambridge, UK, 2018.
82. Selby, M.J. *Landforms of the Subtropics and Tropics, Earth’s Changing Surface*; Oxford University Press: Oxford, UK, 1985.

Disclaimer/Publisher’s Note: The statements, opinions and data contained in all publications are solely those of the individual author(s) and contributor(s) and not of MDPI and/or the editor(s). MDPI and/or the editor(s) disclaim responsibility for any injury to people or property resulting from any ideas, methods, instructions or products referred to in the content.